

Plasma Electron Collection Through Biased Slits in a Dielectric

M.R. Carruth Jr.*

NASA Marshall Space Flight Center, Huntsville, Alabama

A large number of experimental and analytical efforts have been directed toward understanding the plasma sheath growth and discharge phenomena which lead to high-voltage solar array/space plasma interactions. An important question which has not been addressed is how the voltage gradient in the plasma sheath near the surface of such an array may affect these interactions. The purpose of the experimental study described in this paper is to examine the merging of the sheaths around biased slits in a dielectric and how this affects the collection of electrons through these slits. The data, which are obtained by emissive probes and direct measurement of the current collected through the slits, indicate that when the sheaths merge the current collection by the slits is significantly altered with the most positive slit collecting more electrons than it otherwise would. Therefore, the effect of a voltage gradient in the sheath around a solar array should be considered when evaluating solar array performance.

Nomenclature

- a = effective hole radius or slit half-width
- d = slit separation; center to center
- E = electric field
- e = electron unit charge
- r = radial component of cylindrical coordinate system
- x = coordinate perpendicular to slit axis and z ; Cartesian coordinate system
- z = coordinate axis perpendicular to plane of test article
- α = characteristic length for potential change on z axis
- λ = characteristic length for potential change on r or x coordinate
- ϕ = electric potential

Introduction

MOST U.S. spacecraft to date have used low-voltage solar arrays, normally generating a few hundred watts near 30 V. Future large systems will require increasing power generation capability, and as power levels increase, the mass, I^2R power loss, and power distribution system complexity penalties for maintaining low solar array voltages become prohibitive, making higher-voltage array designs mandatory.¹ Thus, it is necessary to thoroughly understand high-voltage solar array operation in the conductive space plasma environment.

Solar array systems consist of strings of solar cells with metallic interconnects between them. These interconnects are at voltages depending upon their positions in the array circuit and are usually exposed to the space environment. When such systems are placed in orbit, they will interact with the naturally occurring space plasma, which may produce power loss from parasitic currents through the plasma and arcing on the array.^{1,2} Both of these interactions are plasma density dependent and present greater hazards at higher densities. The low temperature ionospheric plasma has a peak density on the order of 10^6 particles/cm³ at about 300 km altitude. High-voltage system/plasma interactions will, therefore, be

most severe in low-Earth orbits. The power levels envisioned for future, large spacecraft drive the design toward higher solar array operating voltages. When the spacecraft exits eclipse, this voltage will be even higher until the array warms to normal operating temperature. Successful design of higher-voltage arrays relies on understanding the limits imposed by plasma interactions.

It has been shown that at voltages greater than approximately +100 V, the electron current collected by the solar array increases dramatically.^{1,3} Even though the solar array surface is dielectric, it becomes highly positive and collects current as though it were a conductor. The explanation appears to be that as the plasma sheath grows around exposed interconnects or pinholes, the accelerated electrons strike the dielectric, and low-energy secondary electrons are released and collected by the exposed metal.^{1,4} This leaves the dielectric cover glass positive, allowing the plasma sheath to grow over the solar cells.^{1,4} As the voltage on the array segment and the effective collection area increase, the amount of current collected rises. This current flow through the plasma is not available to the spacecraft and, therefore, represents a power loss to this plasma shunt. Depending on the solar array voltage, the power loss can be substantial and can seriously impact array performance.

In most ground tests, a uniform voltage has been impressed on test samples and the collected charged particle current from the plasma measured. However, for a solar array which is generating its own voltage by having solar cells placed in series, there will be voltage gradients on the surface of the cells and within the surrounding plasma sheath due to difference in voltage between cells. The gradients may be quite high if the cells are strung such that solar cells at considerably different voltages lie next to each other. The electric field structure in the plasma sheath may be complex due to solar cell layout and may influence charged particle collection. If electrons, influenced by the voltage gradient, are actually collected at the higher positive potentials, the power loss will increase accordingly.

The collection of charged particles from the plasma and determination of how this affects solar array performance is a complex problem.⁵ It may be complicated by how voltage gradients on a solar array surface affect charged particle collection. A previous study by Suh et al. addressed whether surface potential gradients on solar arrays in geostationary orbit conditions might affect solar array performance.⁶ Their conclusion was that the surface gradient will affect electron collection, but the magnitude of the currents in

Received Jan. 13, 1986; revision received March 31, 1986. Copyright © 1986 American Institute of Aeronautics and Astronautics, Inc. No copyright is asserted in the United States under Title 17, U.S. Code. The U.S. Government has a royalty-free license to exercise all rights under the copyright claimed herein for Governmental purposes. All other rights are reserved by the copyright owner.

*Space Scientist, Magnetospheric Physics Branch, Space Science Laboratory.

these plasma conditions are small enough so that their impact on array performance is negligible. Because of the much higher plasma densities in low-Earth orbit relative to geosynchronous orbit, voltage gradients on the solar array surface may affect array performance. Some previous experimental investigations were performed in which voltage drops existed in a solar array segment or simulated solar array.^{7,8} These were primarily intended to investigate the floating equilibrium condition for a solar array with a distributed voltage immersed in a plasma. There has been no previous examination of plasma sheath growth around or charged particle collection from a plasma of ionospheric density by solar array or pinholes when a voltage gradient is present. This paper reports on experimental work addressing this subject.

Theoretical Background

Experimental work regarding charged particle collection by both pinholes in dielectrics and segments of photovoltaic cells has been performed.^{1-4,7-9} The pinhole investigations have been conducted in order to understand the physics involved in charged particle collection by high-voltage solar arrays immersed in a plasma. The first experiments to examine high-voltage solar array/space plasma interactions and identify an anomalously high electron collection were performed by Cole et al. and Kennerud.^{10,11} A large number of subsequent experiments investigated the same phenomenon and tried to determine the cause for the large current collection for samples biased positively of the ambient plasma and to determine the effect such current collection has on solar array performance.

Data on current collection and surface potential of both biased solar array segments and pinholes in dielectric material covering biased electrodes indicate that the plasma sheath grows over the dielectric surface for positive potential relative to the plasma. This is observed not to be the case for negative potentials when ions are collected.³ It has been postulated that as the sheath begins to grow around the exposed metal, incoming electrons strike the dielectric surface and low-energy, secondary electrons are released and collected, leaving the surface positive. Analytical examination of charged particle collection by pinholes provides qualitatively correct comparison with experiment.^{9,12-14} A key to these analytical examinations is consideration of secondary electron production. The work of Brandon et al.,¹² Kessel et al.,¹³ and Mandell and Katz¹⁴ deal primarily with lower voltage and the onset of the secondary electrons being a significant current contributor to biased pinholes, while Stillwell et al.⁹ concentrate on high voltage. According to Brandon et al., as the sheath begins to extend into the plasma and onto the dielectric, charged particle collection is enhanced by charge focusing.¹² As the pinhole voltage increases, the current contribution due to secondary electrons becomes the dominant factor. Stillwell et al. point out another mechanism which additionally enhances pinhole electron current collection at higher voltages.⁹ It is associated with vaporization and ionization of the dielectric material at the pinhole edge.⁹

Previous work has been associated with a single bias voltage on a single pinhole or segment of solar cells. In order to determine the effects of a voltage gradient, multiple exposed conductors at different voltages surrounded by dielectric must be examined. If the sheaths which develop around the exposed conductors overlap, then a potential gradient will exist across the surface and within the sheath. Electrons which would have been collected at a lower potential will be collected at a higher potential.

In order to predict how charged particles are collected for multiple pinholes or openings in insulation, the plasma sheath structure must be known. The only experimental examination of sheath structure around pinholes was performed by Gabriel et al.¹⁵ They determined that simple

Debye shielding cannot describe the sheath structure but that it may be satisfactorily described as having an exponential drop-off with characteristic lengths in the z and r axes where the r axis is radially across the dielectric surface from the pinhole and the z axis is perpendicular to the dielectric surface. Mandell and Katz used their NASCAP/LEO model to compare with this experiment and found qualitatively reasonable comparison.¹⁴ According to Gabriel et al., the potential structure may be described by the semiempirical formula

$$\phi(r, z) = \frac{2\phi_0}{\pi} \tan^{-1} \left[\frac{a}{z} \exp\left(-\frac{z}{\alpha}\right) \right] \exp\left(-\frac{r^2}{\lambda^2}\right) \quad (1)$$

where ϕ_0 is the potential applied to the exposed electrode in the pinhole.¹⁵ Even though this formula is semiempirical, it is in closed form and easy to apply to the sheath around multiple pinholes.

A simpler geometrical arrangement to consider is illustrated in Fig. 1. Instead of pinholes, slits in a dielectric covering electrodes are considered. The potential at any point is the sum of the potentials due to each slit. In this case,

$$\phi(x, z) = \frac{2\phi_1}{\pi} \tan^{-1} \left[\frac{a}{z} \exp\left(-\frac{z}{\alpha_1}\right) \right] \exp\left(-\frac{x^2}{\lambda_1^2}\right) + \frac{2\phi_2}{\pi} \tan^{-1} \left[\frac{a}{z} \exp\left(-\frac{z}{\alpha_2}\right) \right] \exp\left[-\frac{(d-x)^2}{\lambda_2^2}\right] \quad (2)$$

The values of ϕ , a , α , and λ are experimental parameters. Values of $\phi_{1,2}$ are set by the experiment. The values of a , α , and λ must be found by experimentally obtaining values of $\phi(x, z)$.

Using the experimental geometry described above, change in $\phi(x, 0)$ indicates the energy with which electrons are accelerated to the surface. Whether they are collected by one exposed conductor or the other depends on the x axis electric field component given by the derivative of Eq. (1) with respect to x . Examination of $E(x, z)$ shows that there is a mild dependence of $E(x, z)$ on z but that it is dominated by x . $E(x, z)$ may be used to find the point at which the x axis component of the electric field is zero, or where the x axis component of the electric field direction reverses. If this field reversal point is between the two slits, it will establish the boundary which will determine that charged particles entering on one side of it will be collected by one slit and those entering on the opposite side will be collected by the other. If the potential difference and proximity of the slits are such that the field reversal point is at or near one of the slits, all the charged particles entering between the slits may be collected by the higher-potential slit.

As the plasma sheath develops around each individual slit, the sheaths are independent. If the potential on an individual slit is raised such that the sheath boundary extends beyond the point halfway between the two slits, a certain amount of

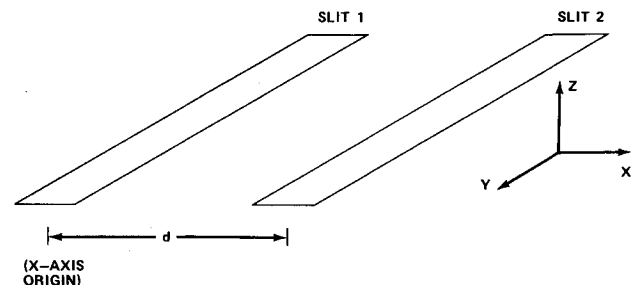


Fig. 1 Slit geometry used in experiment.

current is collected. If the potential on the second slit is raised until the sheaths overlap, the charged particles collected by the high-potential slit will include charged particles that would have been collected by the lower-potential slit.

Experimental Apparatus

The apparatus for this experiment consists of a vacuum chamber, plasma source, plasma diagnostics, and test articles. The steel vacuum chamber is approximately 1 m diameter by 2 m in length. Two 12-in. diffusion pumps provide a pressure of approximately 1.0×10^{-6} Torr when the plasma source is not operating. The background neutral pressure is maintained in the 10^{-5} Torr range during plasma source operation; its exact value is dependent on the gas flow rate through the plasma source.

The plasma source chosen is a hollow cathode which is based on the design reported by Kaufman and Robinson¹⁶ and Stillwell et al.¹⁷ A Langmuir probe is used to determine the characteristics of the plasma generated by the plasma source. The probe is placed in the proximity of the test article so that the plasma conditions at the test article are known. The probe consists of a 7.5-cm-long tungsten wire which is 0.051 cm in diameter. The length was chosen to minimize end effects and the diameter ensures the capability of using thick sheath analysis of the probe data. Two emissive probes are used to determine the local potential within the plasma sheath which develops around the slits in the test article. The probes each consist of a loop of wire.

Tungsten/rhenium wire 0.076 mm in diameter and forming a loop 1.5 mm wide and 1.5 cm long is used in this experiment. A current is passed through the wire, heating it to incandescence. If the probe is allowed to electrically float, it will come near plasma potential by thermal emission of electrons. As with the Langmuir probe, a complete current/voltage curve can be obtained and the plasma information determined. Based on the work of Aston and Wilbur¹⁸ and Gabriel et al.,¹⁵ it is sufficient to allow the probe system to float and obtain one curve of the probe voltage as a function of filament current. The current at which the electron saturation point is reached can, therefore, be determined. The probe can then be maintained at this filament current and used to determine local potential relative to chamber ground through a high-impedance electrometer.

In the experiments described in this report, the noted filament currents are obtained and the emissive probe passed through the outer regions of the plasma sheath formed around the slits. This allows a determination of the x axis variation in the sheath potential for the set distances on the z axis of the two probes.

The test article consists of a square, printed circuit board, 15.24 cm on a side, covered with a 2.0-mil Kapton sheet containing open slits. Data were collected on two slit configurations. In one, the slit widths were 0.64 cm and the slit spacing, d , was 3.0 cm. In the other case, the slit widths were 0.32 cm and the slit spacing d was 2.0 cm. The metal electrodes' pattern is shown in Fig. 2. The Kapton sheet with the proper slits is overlaid on the circuit board and is held by small retainers around the Kapton perimeter. The electrical connections are made through the back of the circuit board. Figure 2 also illustrates the slit configuration when the Kapton sheet is applied to the circuit board.

The conductor pattern shown in Fig. 2 facilitates data collection from slits in the Kapton. The electrodes on each end of the center electrodes are maintained at the same potential as their respective center electrode. However, current measurements are obtained only from the center electrodes. This way the data are obtained with a uniform sheath structure along the length of the center electrode and fringing field effects at the ends of the slits do not affect the data. The length of the slit from which current data are collected is 4.22 cm.

Figure 3 indicates the placement of diagnostic probes around the test article. The slit geometry allows the emissive probes to have a small scale length compared to the sheath size. In a circular or spherical geometry, a much smaller, more delicate probe size would be required for the same scale length.

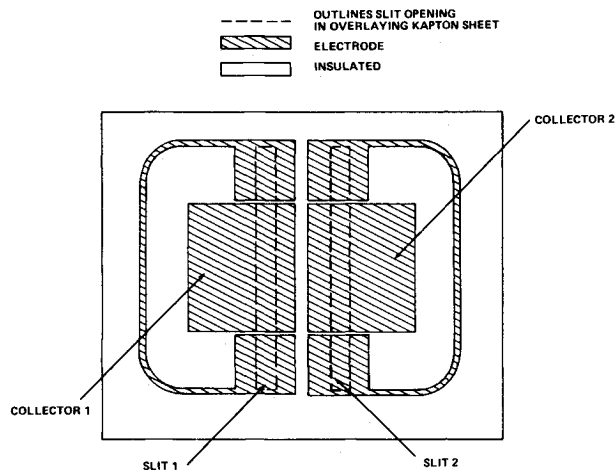


Fig. 2 Diagram of test article used in experiment.

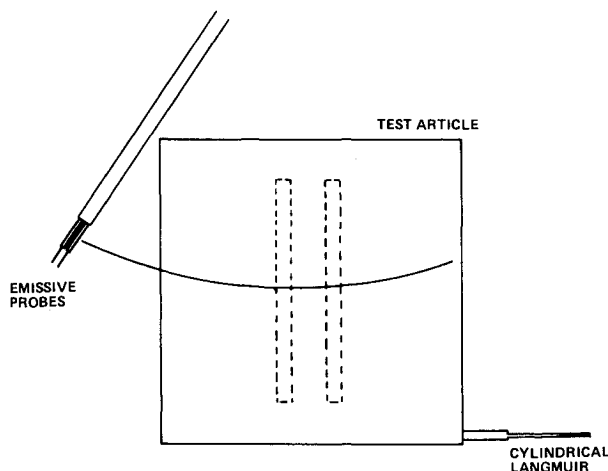


Fig. 3 Illustration of placement of diagnostic probes.

Experimental Results

Plasma Conditions

Data were obtained for slightly different plasma conditions. Repeated operation of the plasma source and collection of data indicate that by setting the plasma source operating conditions, the plasma conditions are reproduced with minimal variation. Data were obtained for Ar gas flows through the source of 7.0–14.0 standard cubic centimeters per minute (SCCM). This variation provided plasma temperatures of 2.0–3.0 eV and plasma densities of from $2\text{--}4 \times 10^6$ electrons cm^{-3} in the vicinity of the test article. It should be noted that the errors expected in determining the density values given are considered to fall within experimental error of each other. Even though the absolute values are not distinguishable, the relative values are apparent because increased current collection by the slits is observed for greater gas flow through the plasma source.

Sheath Structure Around Slits

The emissive probes, previously described, are used to determine the sheath structure around the pair of slits which

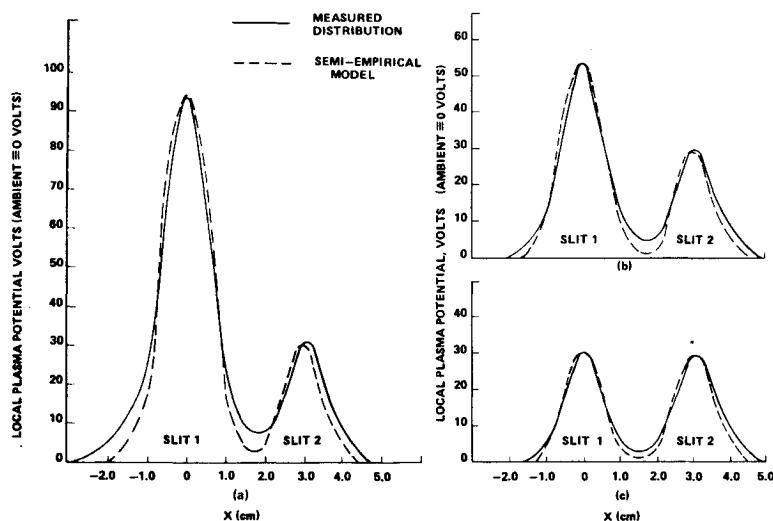


Fig. 4 Potential structure at inner probe location, $z = 0.8$ cm, slit 2 bias = -128 V, slit 1 bias: a) $+328$ V; b) $+228$ V; c) $+128$ V.

are 0.64 cm wide and 3.0 cm apart. These probes will be referred to as the inner and outer probe for the one nearest and farthest, respectively, from the test sample. As already described, the filament current vs probe potential relative to chamber ground is obtained in the plasma near the test sample. The emissive probes reach plasma potential with a filament current of 0.6 A. Therefore, the filament current can be set to 0.6 A and the emissive probe used to measure local plasma potential. Based on the accuracy of the emissive probe technique and the reproducibility of data, the potential measurements given are expected to be accurate to within approximately ± 4 V. Due to the measurement capability, the x axis location at which a potential is specified is accurate to within ± 1.5 mm.

First, the potential structure of the sheath around individually biased slits was measured, and subsequently the structure of the sheath due to biases on both slits was measured. The sheath structure around individual slits is symmetrical about their center. The potential differences between the biased slit and the local plasma is the voltage of importance in considering the plasma sheath structure. The local plasma potential, as obtained by the emissive probes, was always near chamber ground when the plasma source was floating. This was almost always the case; however, some data were obtained without the plasma source floating. The slits were biased by power supplies referenced to chamber ground. Therefore, corrections were made so that the sheath voltage data given in this paper represents the voltage between the slit electrode and the local plasma potential. Data for the potential structure at the location of the inner probe are given in Fig. 4. Similar data for the outer probe location are given in Fig. 5. It is evident from this data that the electric fields are strong within the sheath and that the merging of sheaths of the two slits is more evident in the sheath's outer region. The position between the slits where the potential is a minimum defines the x axis electric field reversal point. Electrons which enter the sheath on one side or the other of this point will not likely cross the potential barrier and will be directed by the electric field to the slit on the electron's side of the barrier. It can be seen in the data in Fig. 5 that the position of the potential minimum shifts toward the slit with the lowest bias when the difference in bias between the slits increase.

Gabriel et al. indicated that a value of α and λ can be used to describe the potential structure throughout the sheath.¹⁵ However, the measured values of λ do vary. Re-examination of the data presented by Gabriel et al. indicates that λ varies by about 40% for a Δz of 1.1 cm.¹⁵ The data presented in this study vary more than this. The reason may be the higher

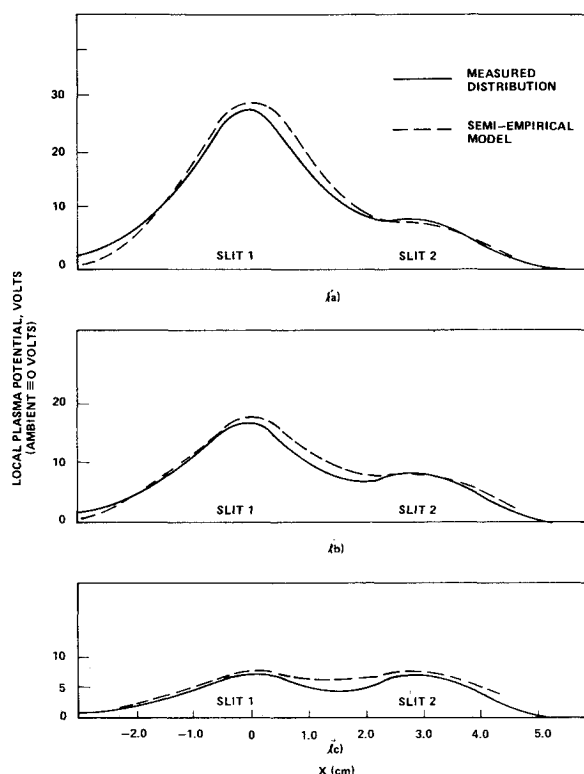


Fig. 5 Potential structure at outer probe location, $z = 1.8$ cm, slit 2 bias = $+128$ V, slit 1 bias: a) $+328$ V; b) $+228$ V; c) $+128$ V.

plasma density of this experiment or effects due to a slit geometry. For a given voltage bias and location in a plane defined by a distance on the z axis, a value of λ can be used to describe the x axis potential distribution. The values of a , α , and λ obtained for a single biased slit are used in Eq. (2) to describe the total potential distribution for the case where both slits are biased. The results of this calculation are also given in Figs. 4 and 5. As indicated by the figures, the potential structure can be described by Eq. (2), with the limitations cited. Table 1 gives values of a , α , and λ used in Figs. 4 and 5.

Electron Current Collection

The sheath structure was examined for single biased slits and for both slits biased. Data were also obtained of the

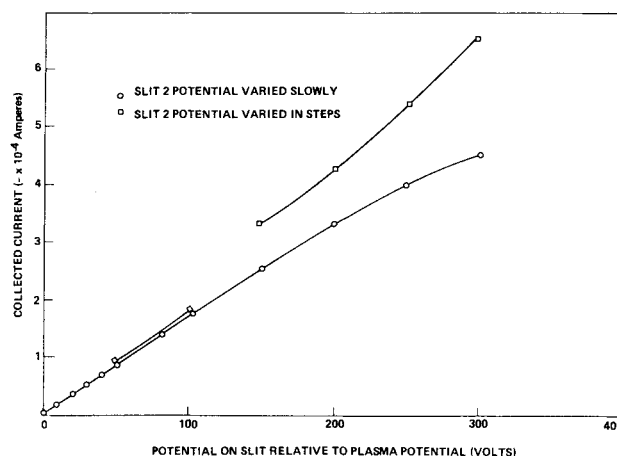
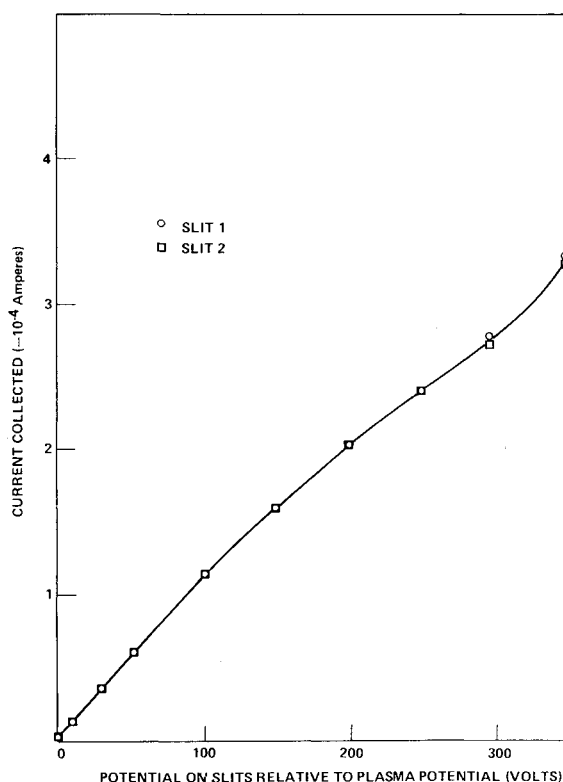
Table 1 Experimental values of a , α , and λ

Volts and position	a , cm	α , cm	λ , cm
+128 V	0.51	1.55	
$z = 0.8$ cm			0.70
$z = 1.8$ cm			1.62
+228 V	0.40	2.98	
$z = 0.8$ cm			0.77
$z = 1.8$ cm			1.56
+328 V	0.53	2.47	
$z = 0.8$ cm			0.81
$z = 1.8$ cm			1.45

electron current collected by the conductor exposed in the slit. The data presented in this report are individual data sets, rather than averaged values. The data sets were reproducible overall to within approximately 20% by resetting plasma source flow rate and discharge current.

For data obtained at any one time and set of experimental conditions, the current collection data were much more reproducible at lower voltages on the slits, normally to within a few percent. It was observed that as voltage on the slit is slowly increased to near 250–300 V, the collected current dramatically “steps” to a higher value, as though a different collection mode existed. This was observed by Gabriel et al. in their pinhole examinations.¹⁵ It is not clear if this mode change is related to the vapor-enhanced collection mode described by Stillwell et al.⁹ or some other effect. In general, the data obtained at these higher potentials at any one time are reproducible to within approximately 10% when the “step” has not occurred. For consistency, the data on current collection, when both slits are biased, are acquired only when this step transition has not occurred. To illustrate this transition effect, the voltage applied to the individual slits was both slowly increased and increased in abrupt steps. Figure 6 represents data for an individually biased 0.64-cm slit. With step voltage increases, the transition to the higher collection mode occurs between +100 V and +150 V. Figure 7 represents data for an individually biased 0.32-cm slit where this transition has not occurred.

In order to determine the effects a voltage gradient in the sheath has on current collection by the two slits, data were collected for various cases where both slits were positive of the ambient plasma and where a potential difference between the two slits existed. This was accomplished by biasing one of the slits by a set potential and maintaining it. The potential on the other slit was then continually increased and the current collected independently by both slits was obtained for the various potentials. These data are presented in Figs. 8 and 9 for the 0.64-cm and 0.32-cm slits, respectively, at an 8.5 SCCM gas flow rate through the plasma source. It can be seen that the current collected by each slit when they are biased +200 V is not the same. It is not clear if this is due to experimental error or is a true difference. This potential is near where the previously described transition to a different collection mode appears to take place. It is possible that the slightly different currents is somehow related to this transition. In the following data presented in this paper, slit 1 is always held at a constant potential and the potential varied on slit 2. It is observed that as the slit 2 potential is increased from zero, the current collected by slit 1 increases. As the potential on slit 2 increases to a value near or exceeding slit 1, the current collected by slit 1 decreases while the current collected by slit 2 increases. The data may be best interpreted by referring to the figures of the plasma sheath structure. As expected, when the bias on both slits is the same, the minimum potential and the electric field reversal point lay exactly between the two slits. As the bias on one of the slits increases, the minimum potential point and electric field reversal point move toward the slit with the lower potential.

**Fig. 6** Individually biased 0.64-cm slit.**Fig. 7** Individually biased 0.32-cm slit.

Therefore, electrons which would have been collected by this slit are now collected by the higher-potential slit.

Because the electron collection is dependent on where the electron enters the sheath relative to the electric field reversal point, the sheath potential curves at the 1.8-cm z axis position are of most interest. In Fig. 5, the electric field reversal point is still distinguishable for the case of one slit bias about +228 V and the other +128 V. However, for the case of one slit bias about +328 V and the other maintained at +128 V, this point is becoming indistinguishable and one expects the amount of current collected by the higher-potential slit to increase. Indeed, this can be seen in the data. Figure 4 indicates that slightly deeper in the sheath, the electric field reversal point still becomes distinguishable. This still becomes a barrier but the electrons entering the sheath are initially drawn to the higher potential. A steeper gradient and/or an increase in potential of both slits relative to the

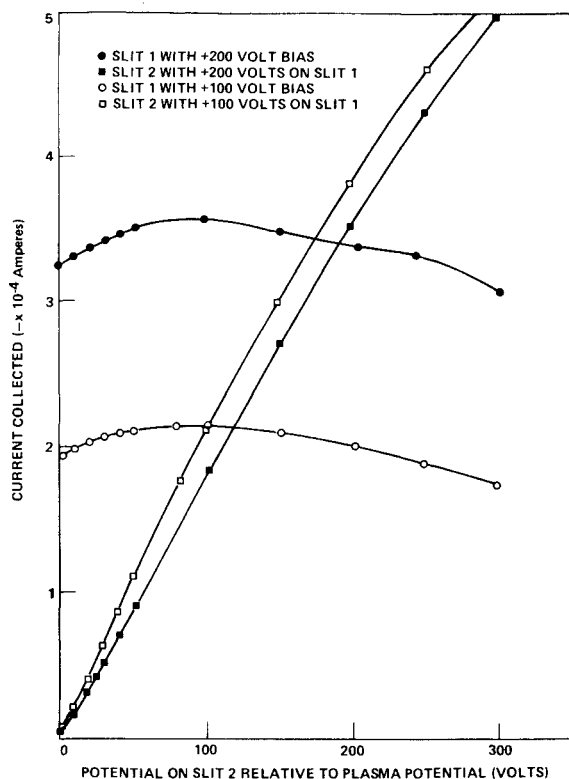


Fig. 8 Current collected with two slits biased, slit size = 0.64 cm, $d = 3.0$ cm.

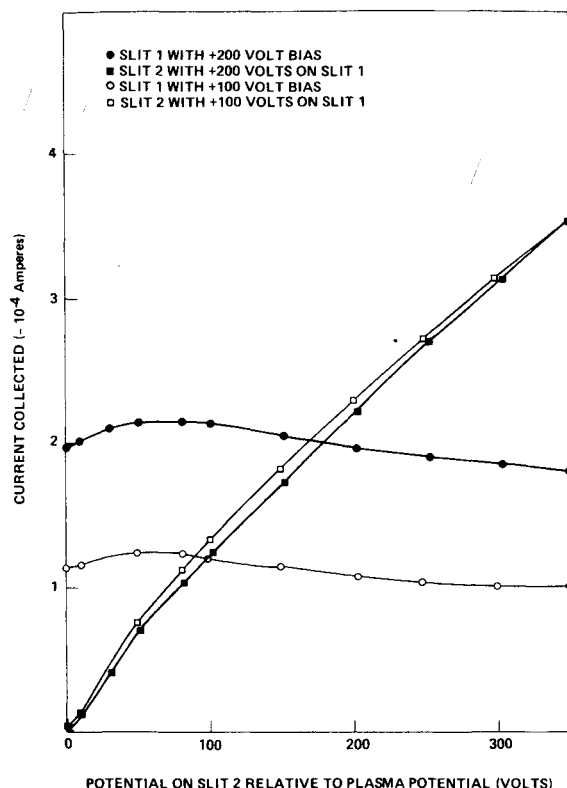


Fig. 9 Current collected with two slits biased, slit size = 0.32 cm, $d = 2.0$ cm.

plasma potential will result in even more current collection by the higher-potential slit at the expense of the one at lower potential. An examination of the data given in the figures reveals that the current collected by slit 2 at a specified high potential is greater when slit 1 is at +100 V as opposed to +200 V.

For all the cases where the potential on slit 1 was set to +100 V, its collected current did not decrease until the potential on slit 2 was increased to above +100 V. However, for the cases where the potential on slit 1 was set at +200 V and the other varied, the current collected by slit 1 at +200 V began to drop well before slit 2 was brought up to +200 V. A possible explanation for this observation is given. With slit 1 set at a specified potential, the potential of slit 2 is increased from zero, at which time there is little or no sheath around it and it cannot contribute current to the slit held at constant potential. As the potential on slit 2 is increased, the sheath around it begins to grow and merge with the sheath from the slit with constant potential and, therefore, only then is additional current made available and supplied to slit 1. As the potential is increased on slit 2, the electric field reversal point between them moves toward slit 1 and the current collected by it begins to decrease. For set distances between the slits, the sheaths are larger for the constant +200 V potential relative to the +100 V potential. Therefore, the effect of the movement of the field reversal point is more pronounced for the case of higher potential and, therefore, the current starts dropping sooner.

The current collected by individual slits is observed to be a linear relationship with potential relative to the plasma. This is consistent with the large pinhole experiments of Gabriel et al.¹⁵ and Kennerud.¹¹ In the introduction to this paper, it was stated that large increases in current have been reported to occur for positive potentials greater than +100 V. However, this was generally for small defects or pinholes.¹¹ The larger sizes in this experiment were chosen to ensure sheath expansion at modest potentials.

Conclusions

The experimental data indicate that a voltage difference between two biased slits in a plasma where their respective sheaths begin to overlap leads to an increase in electron current collection by the one with higher positive potential. Even for small potential differences, it is noticeable; and, for differences of several tens of volts per centimeter, the effect is significant. The electron collection by the most positive slit increases as the condition where the x axis electric field reversal point moves toward the slit with lower potential and ultimately disappears or is prominent only deep within the sheath. For given positive biases, the total current collected by both slits when their sheaths have merged is approximately that collected by the slits biased independently.

The semiempirical formulation for the sheath structure given by Gabriel et al. may be used to calculate the potential and electric field distribution about biased multiple pinholes or slits. However, it is limited by the fact that experimental parameters, obtained from a single slit, must be input, and some parameters identified as constants actually vary with position. This restricts the extrapolation to regions where data are not obtained.

The question of what is the solar array power loss due to the collection of charged particles from the plasma is a difficult one to answer because of the complexity of the current collection and how it affects array performance. The role played by charged particle transport due to voltage gradients on the array and in the surrounding sheath is in itself very complex, but some general conclusions as to its importance may be stated. If the potential difference between solar cells in an array can be maintained such that everywhere strong gradients do not exist and the sheath maintains a "bumpy" potential distribution (electric field reversal on x axis), then the effects of such gradients will probably have a small effect on array performance. If this is not the case, then these gradients may significantly add to the solar array power loss.

The results of the study reported herein indicate that consideration should be given to the effects these surface potential variations will have on solar array performance.

References

- ¹Stevens, N.J., "Interactions Between Spacecraft and the Charged Particle Environment," *Spacecraft Charging Technology—1978*, NASA CP-2071, 1979, pp. 268-294.
- ²Grier, N.T., Smith, C., and Johnson, L.M., "Plasma Interactions with Solar Arrays at High Voltages," *Spacecraft Charging Technology—1980*, NASA CP-2182, 1981, pp. 922-930.
- ³Stevens, N.J., "Investigation of High Voltage Spacecraft System Interactions with Plasma Environments," AIAA Paper 78-672, 1978.
- ⁴Stevens, N.J., "Large Space System-Charged Particle Environment Interaction Technology," NASA TM-79156, May 1979.
- ⁵Domitz, S. and Kolecki, J., "Effect of Parasitic Plasma Currents on Solar-Array Power Output," *Spacecraft Charging Technology—1978*, NASA CP-2071, 1979, pp. 358-375.
- ⁶Suh, P.K. and Stauber, M.C., "Photoelectron Drift and Multiplication Due to Surface Potential Gradient; Application to Solar Power Arrays," AIAA Paper 80-0044, Jan. 1980.
- ⁷Grier, N., "Experimental Results On Plasma Interactions With Large Surfaces at High Voltages," NASA TM-81423, Jan. 1980.
- ⁸McCoy, J.E. and Konradi, A., "Sheath Effects Observed in a 10 Meter High Voltage Panel in Simulated Low Earth Orbit Plasma," *Spacecraft Charging Technology—1978*, NASA CP-2071, 1979, pp. 315-340.
- ⁹Stillwell, R.P., Robinson, R.S., and Kaufman, H.R., "Current Collection from the Space Plasma through Defects in Solar Array Insulation," *Journal of Spacecraft and Rockets*, Vol. 22, Nov.-Dec. 1985, pp. 631-641.
- ¹⁰Cole, R.K., Ogawa, H.S., and Sellen, J.M. Jr., "Operation of Solar Cell Arrays in Dilute Streaming Plasmas," AIAA Paper 69-262, March 1969.
- ¹¹Kennerud, K.L., "High Voltage Array Experiments," NASA CR-121280, 1974.
- ¹²Brandon, S.T., Kessel, R.L., Enoch, J., and Armstrong, T.P., "Numerical Simulations of Positively-Biased Probes and Dielectric-Conductor Disks in a Plasma," *Journal of Applied Physics*, Vol. 56, Dec. 1984, pp. 3215-3222.
- ¹³Kessel, R.L., Murray, R.A., Hetzel, R., and Armstrong, T.P., "Numerical Simulation of Positive-Potential Conductors in the Presence of a Plasma and a Secondary-Emitting Dielectric," *Journal of Applied Physics*, Vol. 57, June 1985, pp. 4991-4995.
- ¹⁴Mandell, M.J. and Katz, I., "Potentials in a Plasma Over a Biased Pinhole," *IEEE Transactions on Nuclear Science*, Vol. NS-30, Dec. 1983, pp. 4307-4310.
- ¹⁵Gabriel, S.B., Garner, C.E., and Kitamura, S., "Experimental Measurements of the Plasma Sheath Around Pinhole Defects in a Simulated High Voltage Solar Array," AIAA Paper 83-0311, 1983.
- ¹⁶Kaufman, H.R. and Robinson, R.S., "Inert Gas Thrusters," NASA CR-165332, Dec. 1980.
- ¹⁷Stillwell, R.P., Robinson, R.S., Kaufman, H.R., and Capp, R.K., "Experimental Investigation of an Argon Hollow Cathode," AIAA Paper 82-1980, Nov. 1982.
- ¹⁸Aston, G. and Wilbur, P.J., "Ion Extraction from a Plasma," *Journal of Applied Physics*, Vol. 52, April 1981.

From the AIAA Progress in Astronautics and Aeronautics Series

THERMOPHYSICS OF ATMOSPHERIC ENTRY—v. 82

Edited by T.E. Horton, The University of Mississippi

Thermophysics denotes a blend of the classical sciences of heat transfer, fluid mechanics, materials, and electromagnetic theory with the microphysical sciences of solid state, physical optics, and atomic and molecular dynamics. All of these sciences are involved and interconnected in the problem of entry into a planetary atmosphere at spaceflight speeds. At such high speeds, the adjacent atmospheric gas is not only compressed and heated to very high temperatures, but strongly reactive, highly radiative, and electronically conductive as well. At the same time, as a consequence of the intense surface heating, the temperature of the material of the entry vehicle is raised to a degree such that material ablation and chemical reaction become prominent. This volume deals with all of these processes, as they are viewed by the research and engineering community today, not only at the detailed physical and chemical level, but also at the system engineering and design level, for spacecraft intended for entry into the atmosphere of the earth and those of other planets. The twenty-two papers in this volume represent some of the most important recent advances in this field, contributed by highly qualified research scientists and engineers with intimate knowledge of current problems.

Published in 1982, 521 pp., 6×9, illus., \$35.00 Mem., \$55.00 List

TO ORDER WRITE: Publications Dept., AIAA, 1633 Broadway, New York, N.Y. 10019